Vertical Profiles of Ozone Concentrations in the Lower Troposphere Downwind of New York City during LISTOS 2018-2019

Maxim H. Couillard[1], M. J. Schwab[2], James J. Schwab[2], Cheng-Hsuan (Sarah) Lu[2,3], Everette Joseph[4], Brennan Stutsrim[1], Bhupal Shrestha[5], Jie Zhang[2], Travis N. Knepp[6], and Guillaume P. Gronoff[6]

[1]Department of Atmospheric and Environmental Sciences, University at Albany, State University of New York, Albany, NY, USA, [2]University at Albany Atmospheric Sciences Research Center, University at Albany, State University of New York, Albany, NY, USA, [3]Joint Center for Satellite Data Assimilation, Boulder, CO, USA [4]National Center for Atmospheric Research, Boulder, CO, USA, [5]New York State Mesonet, University at Albany, State University of New York, Albany, NY, USA, [6]NASA Langley Research Center, Hampton, VA, USA

Corresponding author: Margaret Schwab (jschwab2@albany.edu)

Key Points:

- Vertical ozone profiles below 2 km can exhibit layering unconnected to surface concentrations
- Sea-breeze circulation during stagnation near the land-water interface often induces layering
- Vertical shearing as a result of low-level jets or sea-breeze circulation provides mechanisms for formation of layers

Abstract

Twenty-six balloon-borne ozonesondes were launched near the north shore of central Long Island in the summers of 2018 and 2019 as part of the Long Island Sound Tropospheric Ozone Study (LISTOS). While surface concentrations of ozone are routinely monitored, ozone aloft is infrequently measured, but critical for a full understanding of ozone production and transport. Special attention is given to the lower troposphere from the surface to about 2 km altitude. The observed vertical ozone profiles are presented and analyzed with additional data sources and modeling tools, including LiDAR wind profiles from the New York State Mesonet, back trajectories based on 3 km resolution High-Resolution Rapid Refresh (HRRR) model data, and surface data, aircraft observations, sonde, and ozone LiDAR measurements from other LISTOS participants. The cases analyzed in detail illustrate events with high observed ozone, often with pronounced vertical structure in the profile. Specifically, easily discernable layers are identified with ozone excursions of up to 40 ppbv over short vertical distances. The analysis indicates that meteorological processes can combine to generate the observed vertical profiles. Hot, sunny days with high pressure systems are accompanied by high precursor emissions due to increased power demands, plentiful radiation for photochemistry, and stagnation of synoptic winds. These in turn allow shearing due to meso- and smaller scale flows like low-level jets and sea-breeze/shore-breeze circulation to become dominant and produce the complex vertical layered structure observed. The five cases presented illustrate these processes.

Plain Language Summary

Ground-level ozone pollution is a persistent threat to public health. Ozone increases the risk of heart attack, causes breathing problems, damages lung tissue, triggers asthma attacks, and can even lead to death. Ozone is a secondary pollutant, not directly emitted by humans, but created as a result of our pollutants and chemical reactions. Understanding the meteorology behind high ozone events is important to forecasting and studying unhealthy air quality days. Twenty-six balloon-carried ozone sensors were launched from Long Island in 2018 and 2019 as part of the Long Island Sound Tropospheric Ozone Study (LISTOS). The study identified general patterns leading to high ozone events. We concluded that changes in wind with height led to the high ozone days. Through five case studies, we describe the impacts of small scale, local circulations on ground level ozone. Ozone buildup came from large-scale transport, low-level jets, stagnation

events when the winds were very light for a sustained period of time, and sea-breeze / land-breeze circulations. These situations occur on both the Sound and Atlantic sides of Long Island, bringing in pollutants from the water onto land. This paper illustrates the complex meteorology behind high ozone days in coastal areas near cities.

1 Introduction

Ground-level ozone pollution is a persistent health threat, causing respiratory and cardiovascular illnesses, with even short-term exposure increasing the risk of morbidity and mortality, causing breathing problems, damaging lung tissue, and triggering asthma attacks (Bell et al., 2006; Huang et al., 2005). High levels of ozone are frequently accompanied by elevated air temperatures (Bloomer et al., 2009) with high levels of fine particulate matter ($PM_{2.5}$) and volatile organic compounds (VOCs), as occurred during a July 2018 heat wave (Zhang et al., 2021), further increasing the risk of heart attack, heat stroke, and death (Kinney, 1999). As the climate changes, these episodes are expected to be more frequent and intense (Knowlton et al., 2004; Patz, 2003). The Environmental Protection Agency (EPA) National Ambient Air Quality Standard (NAAQS) Maximum Daily 8-hour Average Ozone level ($MDA8O_3$), set at 70 ppb in 2015, is based on health studies documenting the serious effects of ozone exposure on public health and welfare (USEPA, 2013)Violations of the air quality standards are common in the densely populated urban coastal regions of the Northeast and Mid-Atlantic United States, resulting in the Washington-Baltimore-Philadelphia-New York City Interstate 95 (I95) corridor, and the multi-state region downwind of New York City (NYC) surrounding the Long Island Sound (LIS) being designated EPA nonattainment regions for O_3 (https://www3.epa.gov/airquality/greenbook/phistory_ny.html). It is important to understand and explain the complicated influences leading to high ozone pollution at multiple altitudes in the lower troposphere to 1) inform policy makers, 2) assess compliance to regulations, and most importantly, 3) protect public health.

Ozone is a secondary pollutant formed when precursor nitrogen oxides (NOx) and volatile organic compounds (VOCs) are transformed in the presence of sunlight and water vapor (Godowitch et al., 2008; Goldberg et al., 2014; Loughner et al., 2011). Unraveling the interplay of meteorology, emissions, and chemistry in the formation and transport of ozone is further complicated by the land/water interface where intense urban emissions, urban meteorology, sea

breezes and a lower marine boundary layer may elevate ozone concentrations over short distances (Dacic et al., 2020). This was seen in higher surface levels of ozone over the Great Lakes than over the adjacent land (Levy et al., 2010), and by gradients of over 15 ppb km^{-1} measured near the coast of Long Island (LI) (Zhang et al., 2020). Ozone exceedances frequently occur on hot, cloudless days with stagnant synoptic meteorological conditions and little precipitation. Long residence times of precursors in stagnant polluted air masses allow for the production of high levels of ozone (Naja, 2003; Tawfik & Steiner, 2013). Adding to the complexity of this situation, ozone and other pollutants can be transported great distances along the east coast and over the north Atlantic by low-level jets, narrow bands of relatively fast-moving air disconnected from the surface layer (Hu et al., 2013; Kleiman, 2010; Lee et al., 2011; Stehr et al., 2005).

Ground level ozone and total ozone column are monitored routinely (Lamsal et al., 2015), but stratospheric ozone accounts for most of the total ozone column and obscures the small percentage in the lower troposphere (Fishman et al., 2008). Balloon-borne ozonesondes capture high resolution vertical profiles of O_3 and meteorological data used to identify and characterize layers and air masses in the atmosphere, and to determine whether the ozone and precursors are of local origin or transported from other regions (Thompson et al., 2015). This study reports on a series of balloon-borne ozonesondes deployed by the University at Albany Atmospheric Sciences Research Center (ASRC) during the summers of 2018 and 2019 from the north shore of Long Island in New York State. Below, we present data and additional analyses from a selection of the 18 launches that occurred in 2018 and the 8 launches that occurred in 2019.

2 Materials and Methods

2.1 Long Island Sound Tropospheric Ozone Study

The Long Island Sound Tropospheric Ozone Study (LISTOS) (https://www.nescaum.org/documents/listos) was organized by the Northeast States for Coordinated Air Use Management (NESCAUM) to study the formation and transport of ozone and its precursors, and to characterize the photochemical and meteorological conditions that contribute to exceedance events in urban coastal regions downwind of the New York City metropolitan area. This multi-agency collaboration between government and university researchers combined a host of in-situ and remote sensing techniques on platforms ranging from ground based instruments to satellites

to augment routine monitoring and give a more complete picture of ozone production and concentration, both temporally and spatially.

Deployment dates and times were chosen in collaboration with air quality forecasters and sonde operators on days when the meteorological forecast featured favorable conditions for the formation of moderate to unhealthy levels of ozone. These conditions included, but were not limited to, weak synoptic winds, westerly-southwesterly synoptic winds, broad high pressure, multiple days of clear skies, and high temperatures. Field sites for the ozonesonde deployments were chosen on the north coast of Long Island approximately 80 km downwind of NYC near Stony Brook NY. Figure 1 and Table 1 show the locations of balloon launches and related measurement activity in the NYC metro and Long Island area.

A total of twenty-six balloon-borne meteorological and ozonesondes were deployed by ASRC during the summers of 2018 and 2019 to obtain vertical profiles of ozone, temperature, relative humidity, pressure, and the GPS data from which wind speed and direction are derived. Ozone, temperature, relative humidity, and pressure readings from the sondes were verified against ground-based sensors just prior to each launch. ASRC used an EN-SCI model Z electrochemical concentration cell (ECC) ozonesonde coupled with a Vaisala RS41-SGP meteorological radiosonde. The NASA Langley Research Center (NASA LaRC) sonde flight package consisted of an EN-SCI model 2Z ECC ozonesonde coupled with an iMet-1-RS meteorological sonde. All ozonesondes used the 0.5% buffered KI solution which has been shown to produce readings with precision better than ± (3–5)% and an accuracy of ± (5–10)% through the troposphere up to 30 km (Johnson, 2002; Smit et al., 2007).

Figure 1. Map of Long Island NY with field and monitoring sites (see Table 1). Flax Pond and Stony Brook DEC sites from which sondes were launched (stars). NYS Mesonet profiler sites (red squares). NWS stations (circles). NASA LaRC site in Westport CT (triangle).

Table 1 Locations of field and monitoring sites

Organization	Station	Location	Lat	Lon	Elevation	Primary measurement
DEC	Flax Pond Marine Lab	Old Field, NY	40.9610°N	73.1390°W	4 m	O_3 sonde
DEC	NYSDEC Region 1 Office	Stony Brook, NY	40.9215°N	73.1201°W	37 m	O_3 sonde
NYSM	PROF_WANT	Wantagh, NY	40.6502°N	73.5054°W	18 m	Wind LiDAR
NYSM	PROF_STON	Stony Brook, NY	40.9196°N	73.1333°W	55 m	Wind LiDAR
NYSM	PROF_BRON	Bronx, NY	40.8725°N	73.8935°W	59 m	Wind LiDAR
NWS	Mac Arthur Airport (KISP)	Islip, NY	40.79°N	73.1°W	30 m	Meteorology
NASA LaRC	Sherwood Island State Park	Westport, CT	41.1180°N	73.3369°W	3 m	O_3 sonde, O_3 LiDAR

Abbreviations: DEC – Department of Environmental Conservation (New York State), NWS – National Weather Service, NYSM – New York State Mesonet; PROF – Profiler Site, NASA LaRC – National Aeronautics and Space Administration Langley Research Center

2.2 Ozonesonde Launch Sites

2.2.1 Flax Pond Field Site

During the summer of 2018, sondes were deployed from the Flax Pond Marine Lab, located on a tidal marsh on the north shore of Long Island in Old Field, NY (40.9610°N, 73.1390°W), at 4 m above sea level (Fig. 1, Table 1). A site for the New York State Department

of Environmental Conservation (DEC) Ambient Air Monitoring Network was being established at this location. Eighteen ozonesondes and one additional radiosonde were launched between 18 June and 16 August 2018 during six predicted ozone events. Surface measurements of pressure, temperature, and humidity (PTU) were taken with an Onset HOBO Weather Station erected on the DEC roof platform approximately 5 m above the sheltered launch site in front of the building. Surface measurements of ozone were obtained from the DEC Teledyne API Model T400 ozone analyzer operated at the Flax Pond site as part of their Ambient Air Monitoring Network.

2.2.2 Stony Brook Field Site

Due to construction, the Flax Pond Marine Lab was not available in 2019, so a field station was established at the nearby DEC Region 1 Office in Stony Brook, NY (40.9215°N, 73.1201°W), at 37 m above sea level, and 5km south of Long Island Sound. Ten launches occurred from this site during three ozone events in July 2019. For two of the launches, radiosonde data were reported, but ozonesonde data were not due to equipment failures related to high ambient temperatures. A Lufft WS500-UMB Smart Weather Sensor provided the surface PTU measurements. Surface ozone levels were monitored continuously at the site with a TECO Model 49 Ozone Analyzer. Additional measurements came from the Flax Pond DEC analyzer and from the University at Albany Mobile Lab (Zhang et al., 2020, 2021) stationed 2 km south on the Stony Brook campus (40.9039°N, 73.1188°W).

2.2.3 Westport CT Field Site

Westport Sherwood Island State Park (41.1180°N, 73.3369°W) is an ambient air monitoring site operated by the Connecticut Department of Energy and Environmental Protection (https://portal.ct.gov/deep). This is a coastal site in southwestern Connecticut, approximately 0.5 km to the south of I-95 on Long Island Sound. The NASA Langley Research Center (NASA LaRC) launched eleven ozonesondes from this site, and the NASA Langley Mobile Ozone Lidar (LMOL) was stationed here from 12 July to 30 August 2018 (Gronoff et al., 2019; De Young et al., 2017).

2.3 Data and Figures

Sonde profiles consist of data for ozone (O_3 ppb), relative humidity (RH %), virtual potential

178 temperature (Θ_v °K), and boundary layer height (BL) as determined by an increase in virtual
179 potential temperature. Wind barbs indicate wind direction and speed in knots. Back trajectories
180 from the National Oceanic and Atmospheric Administration (NOAA) Hybrid Single-Particle
181 Lagrangian Integrated Trajectory (HYSPLIT) atmospheric transport and dispersion modeling
182 system use archived HRRRV1 3km meteorological data in 2018, and HRRR 3km in 2019 (Stein
183 et al., 2015) (https://www.arl.noaa.gov/hysplit/), and are run for 24 hours except where indicated.
184 The receptor site (usually Flax Pond) is indicated by a star. Receptor heights are chosen to
185 represent points of interest in the O_3 profile. Note that time increases to the left for the trajectory
186 heights at the bottom of each plot. MDA8O_3 air quality maps are from the AirNow archive
187 (https://gispub.epa.gov/airnow/). Yellow indicates an MDA8O_3 between 55 and 70 ppb, orange
188 indicates values between 71 and 85 ppb, red indicates values between 86 and 105 ppb, and
189 purple indicates values between 106 and 200 ppb. Scanning Doppler LiDAR vertical profile
190 curtain plots are from the NYS Mesonet Profiler Network (Brotzge et al., 2020). Horizontal wind
191 direction is indicted by a barb and speed is indicated by color. Plots of vertical winds indicate
192 speed and direction by color, with red as rising and blue as sinking. Sonde launch times are
193 indicated on the curtain plots by black lines. Weather maps are from the NOAA archive (https://
194 www.emc.ncep.noaa.gov/emc/pages/numerical_forecast_systems/gfs.php).
195

196 **3. Results**

197 3.1 Overview

198 2018 was an active year for ozone in the NYC metro area. A total of 19 days with
199 exceedances were recorded by the eleven DEC monitoring stations in this region, and all eleven
200 stations were non-compliant with the ozone NAAQS, having a 4th highest MDA8O_3 above 70
201 ppb. In contrast, there were 11 days with recorded exceedances in 2019, and only three stations
202 were non-compliant for the season that year. The summers of 2018 and 2019 were both hotter
203 than average, with average daily maximum temperatures 27.5 °C and 27.8 °C, respectively,
204 compared to a normal of 26.4 °C. Neither summer was unusually dry, with a rainfall amount
205 within 35 mm of the normal accumulated precipitation amount of 301 mm. Each year had 8 days
206 where maximum temperature exceeded 32.2 °C (90 °F), compared to the normal 4.8 days. The

yearly record high temperature was 35.0 ºC (95 ºF) on 1 July 2018 and 37.2 ºC (99 ºF) on 21 July 2019, both of which were LISTOS launch days.

Table 2 provides a brief overview of the 26 flights described in this paper, which occurred on days when ozone exceedances were predicted in the NYC metro area. The surface ozone mixing ratio measured at launch time is listed, along with the maximum ozone observed in the lowest 2 km of the troposphere during each flight. While there may be interesting and important structure in the ozone mixing ratio at higher altitudes, the analysis in this study focuses on the lowest 2 km. Most high ozone events in this location occurred under the influence of a high pressure system over the southeast US, with weak winds; and the next most common meteorology involved a frontal passage. Not all forecasts of high ozone resulted in exceedances at this central Long Island location, as is obvious in the table for the predicted event of 20-21 July 2019. While there was moderate ozone observed aloft (68 ppb around 550 m) on 20 July, the front moved the high ozone air mass south and east more quickly than expected, and the two flights on 21 July observed low ozone mixing ratios. Figure 2 presents the vertical ozone profiles below 5 km for all 26 flights, indicating the range of observed ozone over this central Long Island location

Dry deposition of ozone results in lower O_3 at the surface, a prominent feature in the vertical profiles in Figure 2 (Clifton, Fiore, et al., 2020; Clifton, Paulot, et al., 2020). The loss is typically greater during the night due to the shallow nocturnal boundary layer and cessation of ozone production. Ozone levels over water have been found to be higher than over the adjacent land due in part to the lower dry deposition rates and shallower boundary layer over water (Goldberg et al., 2014; Qin et al., 2019), and recirculation by bay or sea breezes can bring polluted air ashore, impacting the air quality in coastal regions (Angevine et al., 2004; Dacic et al., 2020).

Table 2

Selected data and descriptive terms for all ozonesonde launches during 2018 and 2019.

Launch number	Launch date	Launch time	Surface O_3	Max O_3 below 2 km	Altitude max O_3 below 2 km	Boundary layer height	Meteorological conditions
Units	*m/d/y*	*UTC*	*ppb*	*ppb*	*m*	*m*	
1	6/18/2018	21:16	56	103	800	400	Bermuda High
2	6/24/2018	19:08	47	72	1250	550	Warm front passage

3	6/30/2018	17:18	48	66	300	1300	Blocking high
4	7/1/2018	5:54	43	63	550	1150	Blocking high
5	7/1/2018	9:59	22	60	1000	1200	Blocking high
6	7/1/2018	17:50	53	60	250	400	Blocking high
7	7/2/2018	6:08	26	75	1150	1200	Blocking high
8	7/2/2018	17:14	61	111	1250	1700	Blocking high
9	7/2/2018	20:10	69	94	550	1550	Blocking high
10	7/10/2018	17:16	81	87	650	1700	Front passage
11	7/10/2018	19:56	117	135	1700	1800	Tropical cyclone to the south
12	8/5/2018	17:25	56	67	2000	1650	High Pressure
13	8/5/2018	20:09	45	58	200	1750	High Pressure
14	8/6/2018	13:02	22	59	1900	250	High Pressure
15	8/6/2018	17:00	75	80	650	1600	High Pressure
16	8/6/2018	19:47	45	83	1300	1700	High Pressure
17	8/15/2018	17:48	53	58	200	1500	Cold front passage
18	8/16/2018	19:48	64	77	550	1500	Cold sector
19	7/10/2019	18:48	48	77	1700	2300	High Pressure
20	7/20/2019	16:03	57	68	550	600	Approaching cold front
21	7/21/2019	5:51	25	55	2000	1600	Approaching cold front
22	7/21/2019	13:44	33	45	400	600	Approaching cold front
23	7/21/2019	17:38	39	48	1000	1000	Approaching cold front
24	7/28/2019	19:54	70	88	1050	2000	High Pressure
25	7/29/2019	14:29	59	63	400	400	High Pressure
26	7/29/2019	19:13	82	102	1300	1900	High Pressure

Date and time of each launch, surface ozone, maximum ozone in the lowest 2000 m of the troposphere and altitude of the maximum ozone in the lowest 2000 m of the troposphere, and the boundary layer height determined from the sounding. The final column briefly describes the meteorology prevalent on launch day.

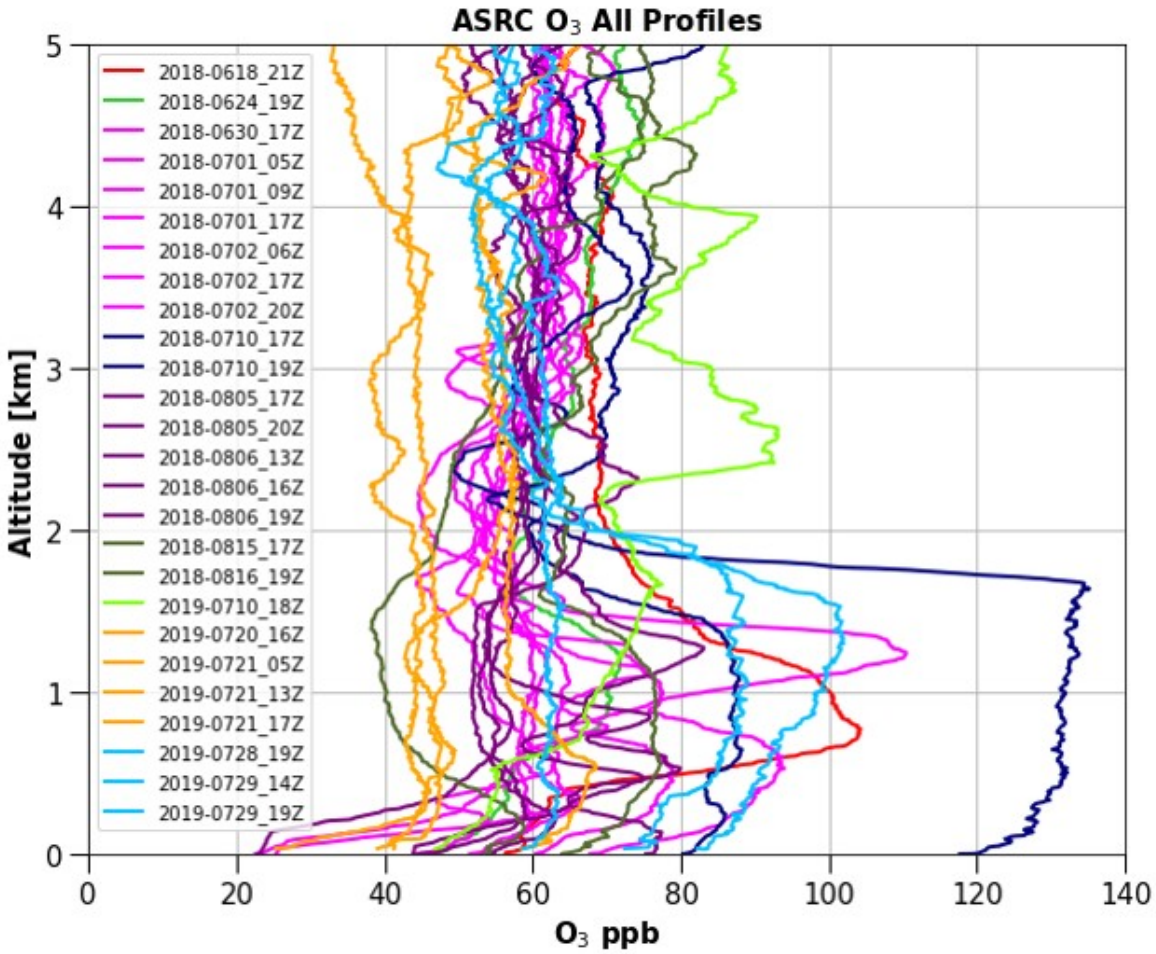

Figure 2. Vertical profiles in the lower troposphere for all ozonesondes launched for LISTOS 2018 and 2019 by ASRC. Profiles for each event are grouped by color. Data for all flights are available at https://www-air.larc.nasa.gov/missions/listos/index.html.

Five case studies are presented in greater detail to explore the observed vertical structure in the ozone mixing ratio. These cases illustrate the influence of stagnation, low-level jets, sea breeze and bay breeze circulation, and the convergence of sea and bay breeze circulation on the ozone mixing ratio and its vertical structure at this central Long Island location.

3.2 Low-Level Jet: 18 June 2018

This event was characterized by an anti-cyclonic high over Alabama, and a cyclone in Northern Quebec creating a strong westerly flow from the Great Lakes to the east coast (Fig. 3a). A cold front was well north of the NY international border, and a warm front moving off the New England coast put LI well into the warm sector, with a temperature of 28 ºC at the 21Z sonde launch. The MDA8O_3 was less than 70 ppb over LI, but between 71 and 85 ppb along the

I95 corridor (Fig. 3b). The zonal flow across PA from Lake Erie contained moderate levels of ozone. A nocturnal low-level jet with 30 kt winds carried these pollutants towards LI. This is visible in the LiDAR (Fig. 3c) as a narrow strip of fast-moving westerly and southwesterly wind 500 m above the surface on the morning of 18 June. Adding to this was the flow originating at the Chesapeake Bay, traveling north at ground level, and being lofted to 700 m to converge with the stream traveling west over LI (Fig. 3d), resulting in an ozone peak of 104 ppb. The 21Z vertical profile (Fig. 3e) shows moderate ground level ozone of 56 ppb at Flax Pond in a shallow boundary layer below 400 m. This stable layer prevented the higher levels of ozone from reaching the surface. This event resulted in ozone exceedances at four LI sites, though not at Flax Pond.

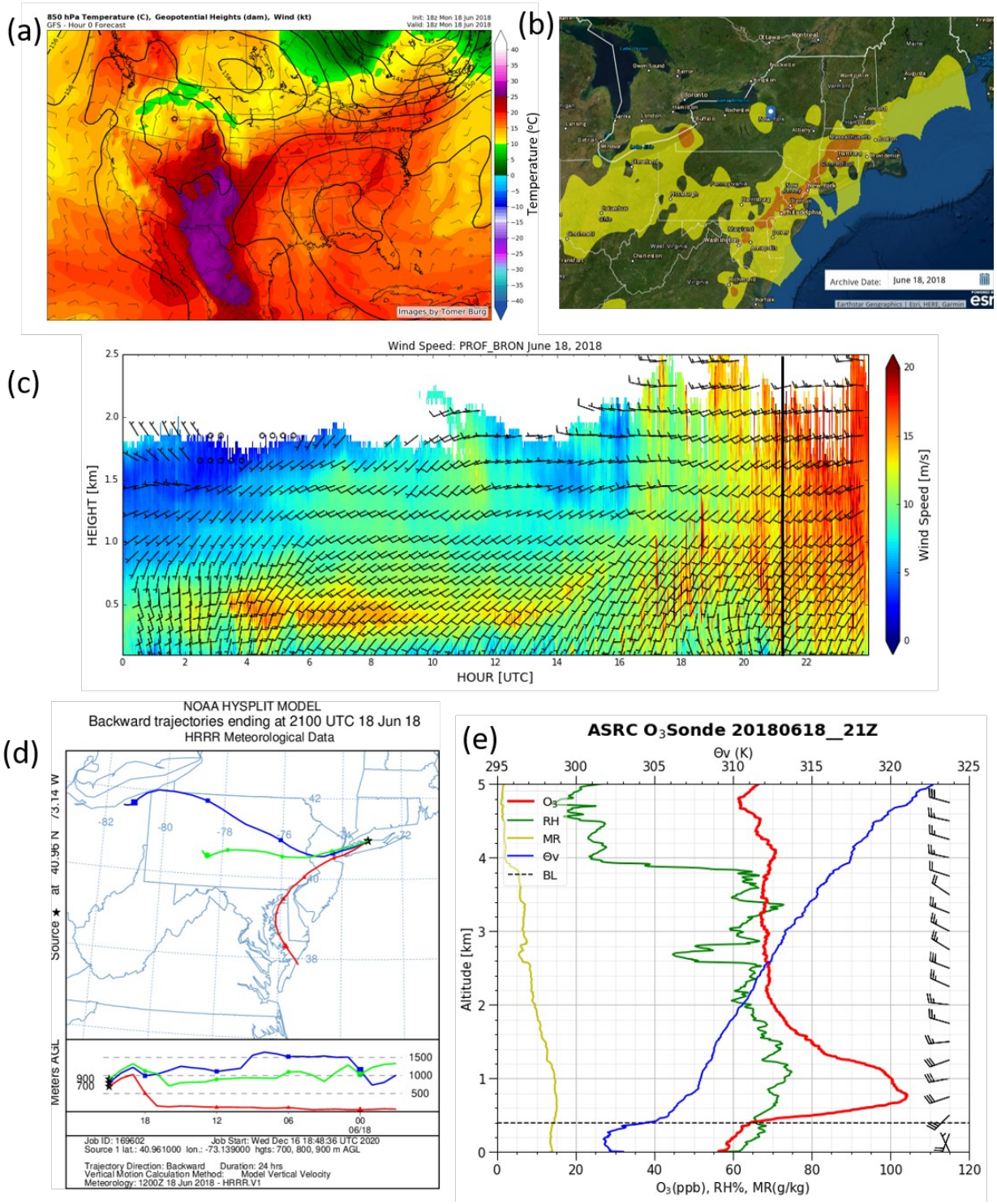

Figure 3. 18 June 2018 event. (a) GFS 850 hPa forecast map for 18 June 2018. (b) MDA8O_3 AQI contours (https://www.airnow.gov/). Colors explained in text. (c) Vertical profile of wind speed and direction measured by NYS Mesonet LiDAR at Bronx, with the 21Z launch indicated by a black line. (d) Back trajectories ending at 21 UTC corresponding to the ozone peak at 700-900 m. (e) Ozonesonde vertical profile for 21Z 18 June 2018. Red - ozone (O_3 ppb), green -

relative humidity (RH %), blue - virtual potential temperature (Θ_v °K), black - boundary layer height (BL). Wind barbs indicate wind direction and speed in knots.

3.3 Sea Breeze Recirculation over Atlantic: 30 June to 2 July 2018

This was the most significant event of the study, with a blocking high pressure region, high temperatures, stagnant winds, and air mass recirculation over the ocean contributing to the ozone exceedance. The primary meteorological condition setting up this multi-day exceedance event was a blocking 1020 hPa high pressure region sitting over PA and WV, with no frontal features within 1000 km of LI for the duration of the event (Figs. S1a, b, c). The 48-hour back trajectories for 30 June and 1 July (Fig. S2a, b) show weak northwesterly, then westerly winds flowing from the Great Lakes through regions with elevated O_3 (Fig. S3), towards NYC. The yearly record high temperature of 35.0 ^oC (95 ^oF) was recorded on 1 July 2018 (NWS Islip), and the 2 July MDA8O_3 reached 115 ppb in Rockland County, north of NYC (Fig. S3). Seven ozonesondes were launched over the three-day period (Table 2).

The extreme temperatures over the mideast and northeast US led to increased pollutant emissions and the weakening winds (increasing stagnation) allowed the multi-day ozone build-up shown in Figure S3. This build-up was not uniform across the whole region, and the interplay of enhanced emissions, weak synoptic flows, and land-water interfaces also created some striking layered ozone vertical profiles during this period (Figs. 4a, b, c).

The Stony Brook wind LiDAR (Fig. S4a) shows that 30 June started with moderate northerly winds which turned to light easterlies by mid-morning before dying around noon. The sonde launched at 17Z on this day (Fig. S5a) measured only moderate ozone levels (60-66 ppb) from 200-1400 m, as the light synoptic flows isolated north central Long Island from the higher ozone to the west in New York City. 1 July was similar in many ways, although there was more of a westerly component to the surface winds and winds aloft overnight, and the overnight sonde at 6Z measured moderate ozone again, but with some layering evident in the lowest 600 m (Fig. S5b). By 10Z the winds weakened and turned northerly and the sonde measured 60 ppb of ozone from 600–1400 m (Fig. S5c). Like on 30 June, the winds started to die down around noon, then turned weak easterly aloft before becoming too weak for a good retrieval. The sonde launched at close to 18Z that day barely measured 60 ppb at 200 m, fell off another 1-2 ppb up to 800 m, then another 13-14 ppb to reach a minimum at 1650 m (Fig. S5d). Again, the pool of higher ozone to the west did not greatly influence the surface ozone nor the ozone aloft.

The LiDAR for 2 July shows the synoptic winds at Stony Brook weakening even more and with a greater westerly component (Fig. S4c). The overnight launch at 6Z (Fig. 4a) shows very low surface ozone, then three layers below 1200 m, increasing from 66 ppb at 350 m to 70 ppb at 88 m, then 75 ppb at 1150 m. The light northwesterly winds gave way to complete stagnation 5-15Z in the lowest kilometer. The stagnation of synoptic winds allowed for the land/sea breeze circulation to become the dominant flow even on the north side of Long Island at Stony Brook as shown in Figure S4c beginning around 15Z. From 1 July 14Z to 2 July 14Z, the drastic weakening of the winds over the ocean allowed for air masses to age and recirculate.

The very high O_3 maximum observed at 1200 m in the 17Z ozonesonde (Fig. 4b) corresponds to the blue trace in the 17 UTC back trajectory (Fig. 4d). This trajectory depicts the air that was over Long Island 24 hours earlier, and then advected out to sea by a nighttime land breeze. This is indicated in the trajectory by the sudden increase in height as the parcel crosses into the Atlantic at 20 UTC, and then gradually descends over the ocean. The stagnant winds allowed the parcel to stay offshore overnight and into the morning of 2 July. The shallow boundary layer over the ocean enhanced O_3 production and concentration. Ozone precursors and the already moderately high ozone levels in the parcel were 'set to cook' in the Atlantic and drastically increased the low-altitude ozone concentration. In the afternoon, a weak southerly sea-breeze flow became the dominant circulation. The back trajectory indicates the parcel rose sharply upon returning over land, additional evidence of the sea breeze circulation. After a 24+ hour stagnation event, the 1200 m parcel returned to LI with an ozone concentration of well over 100 ppb. The elevated ozone layer at 500 m also spent more than 24 hours off shore in the vicinity of the New Jersey / New York Bight as illustrated by the red trajectory trace in Figure 4d. The final launch of this event (Fig. 4c) shows a layer between 70 and 800 m with an ozone concentration approaching 95 ppb. This broad layer is the result of vertical mixing over the Long Island land surface as depicted in the LiDAR vertical wind velocity curtain plot (Fig. 4e). The observed variation of vertical velocity between positive (upward) and negative (downward) wind components between the 17Z and 20Z launches, extending to at least 1 km in height, is hypothesized to have efficiently mixed the two layers observed in the 17Z profile into a single broader layer observed in the 20Z profile.

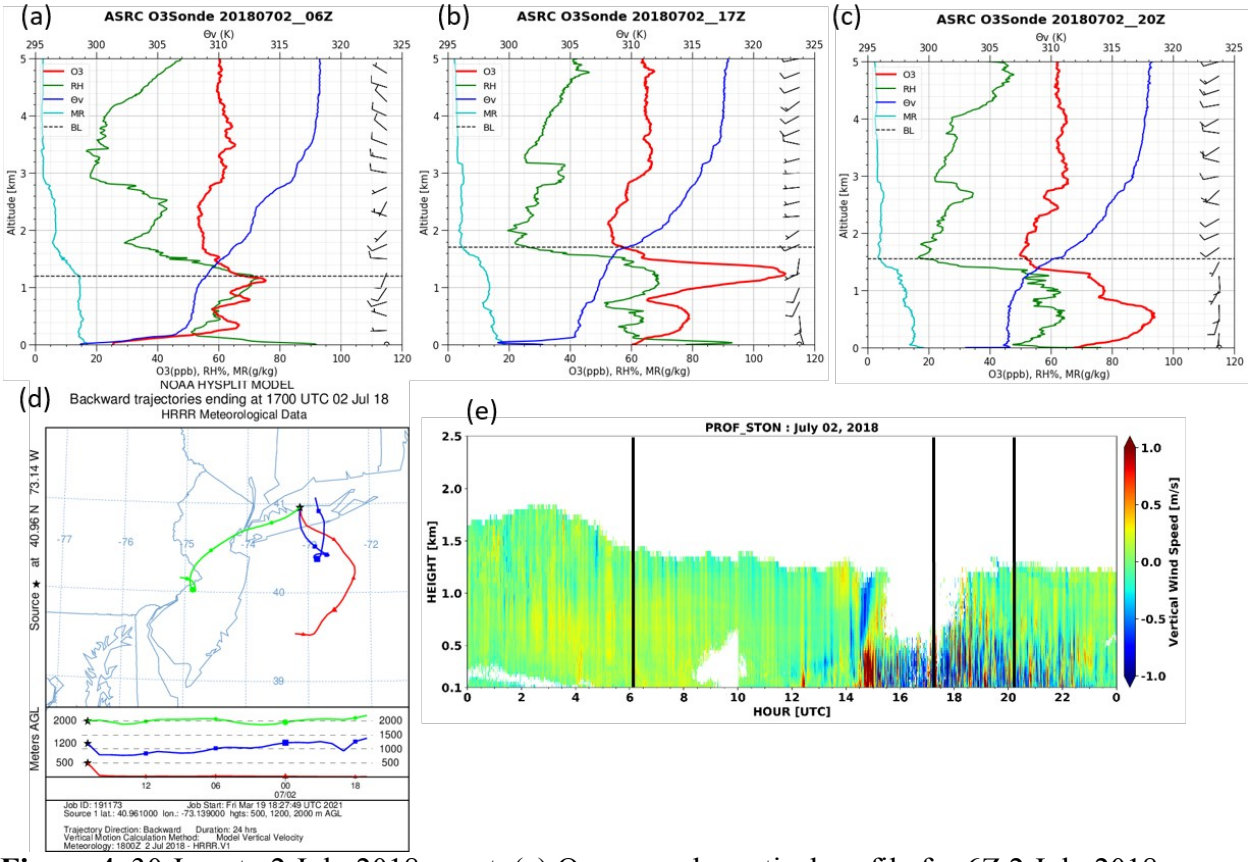

Figure 4. 30 June to 2 July 2018 event. (a) Ozonesonde vertical profile for 6Z 2 July 2018. Colors as in Fig. 3d. (b) Ozonesonde vertical profile for 17Z 2 July 2018. (c) Ozonesonde vertical profile for 20Z 2 July 2018. (d) Back trajectories ending at 17 UTC 2 July 2018. (e) Vertical profile of vertical wind speed measured by NYS Mesonet LiDAR at Stony Brook on 2 July 2018. Black lines indicate launch times.

3.4 Transport over NYC and the Long Island Sound: 10 July 2018

The highest ozone concentrations of the two years occurred on this day, both at the surface and aloft measured by an ozonesonde. At the surface, the Flax Pond site reported 94 ppb as its MDA8O_3, and a 1 hour average maximum value of 124 ppb. As can be seen in Figure 5a the highest MDA8O_3 surface concentrations were observed in a band ranging from western coastal Connecticut, across the Long Island Sound and then encompassing central and eastern Long Island. Two ozonesondes were launched from Flax Pond this day, one just after 17Z and the other just before 20Z (Table 2, Figs. 5b-5c).

There was no significant synoptic regime over LI, with a cold front approaching from the north and tropical storm Chris located off the Carolina Coast (Fig. S6a). The uniform ozone concentrations throughout the mixed layer are evident in both ozone profiles (Figs. 5b-5c); with

ozone near 85 ppb at 17Z and 130 ppb by 20Z. In each of these profiles the ozone above the mixed layer dropped to more moderate values near 60 or 70 ppb. The back trajectory for this case was restricted to 12 hours to show the details near NYC more clearly (Fig. 5d). The lowest layer (red) passed directly over northern NYC where it lofted dramatically before proceeding over LI Sound. It subsided and rapidly mixed downwards over the water between the city and the Flax Pond launch site. The Stony Brook wind LiDAR (Fig. 5e) indicates the winds at this location died down a few hours before the first launch and remained mostly weak until after the later launch. The subsidence combined with the weak ventilation over north central Long Island and light afternoon sea breeze seen in the Wantagh wind LiDAR (Fig. S6b) allowed the build-up of the very high ozone concentrations observed in the profiles.

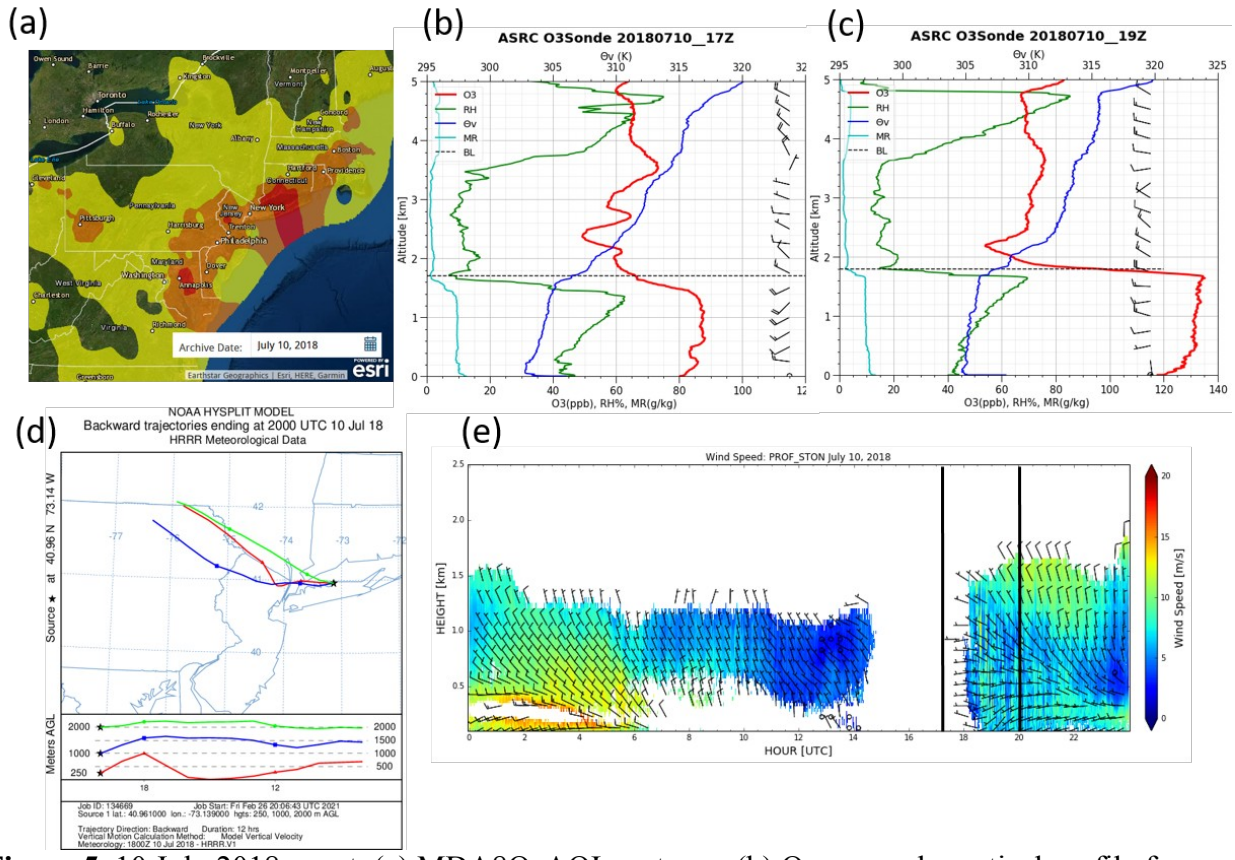

Figure 5. 10 July 2018 event. (a) $MDA8O_3$ AQI contours. (b) Ozonesonde vertical profile for 17Z 10 July 2018. (c) Ozonesonde vertical profile for 20Z 10 July 2018. (d) Back trajectory for 12 hours preceding 20 UTC 10 July 2018. (e) Vertical profiles of horizontal wind speed and direction measured by NYS Mesonet LiDAR at Stony Brook on 10 July 2018. Black lines indicate launch times.

3.5 Stagnation, convergent sea and shore breeze, cross LIS flow: 5-6 August, 2018

The stagnant air over LIS in this event was similar to 10 July 2018 (Fig. 5d), but instead of ozone being well mixed within the boundary layer, the ozone profiles on 6 August (Figs. 6a and 6b) show distinct layers, as were seen on 2 July 2018 (Figs. 4a, 4b, 4c). The satellite image for 6 August 2018 (Fig. 6c) illustrates a phenomenon familiar to Long Island on warm, nearly stagnant summer days, namely the formation of forced fair weather cumulus clouds along the center of Long Island where the Atlantic Ocean sea-breeze and the LIS shore-breeze converge. Note also the corresponding shore-breeze forced cumulus along the southern coast of Connecticut. Wind LiDAR plots confirm the formation of a robust sea-breeze at Wantagh on the Atlantic side (Fig. S7a), and a weaker, but still observable shore-breeze at Stony Brook near the north shore (Fig. S7b).

Additional data were available on 6 August from the Westport, CT site (Fig. 1, Table 1) from the Langley Mobile Ozone Lidar (LMOL) (Fig. 6d) and an EN-SCI Model 2Z ozonesonde attached to an iMet radiosonde (Fig. 6e). Both ozonesonde and LMOL measurements at Westport occurred on various days between 12 July and 30 August during LISTOS, operated by personnel from the NASA Langley Research Center. LMOL is part of NASA's Tropospheric Ozone Lidar Network, and is capable of providing profiles of ozone between 0.1 and 12 km (Farris et al., 2019; Gronoff et al., 2019; De Young et al., 2017).

The effects of water vs. land can be seen clearly in the 20 UTC back trajectory with Flax Pond as the receptor site (Fig. 6f), as the ozone-laden air mass traveling over LIS sinks to 500 m, while that reaching land at 18Z rises to 1200 m. The resulting peaks are prominent features in the ozonesonde vertical profile (Fig. 6b). A third O_3 peak at 2200 m is due to air that has been circulating above the boundary layer over the ocean. Moving across LIS to the coast of CT two hours later, Fig. 6g shows the 12 hour back trajectory with Westport CT as the receptor site at the time of the 22Z ozonesonde launch from that location. The two lower levels at 250 and 500 m show that air impacting the Westport site came off Long Island Sound, and that the air at 250 m crossed Long Island Sound completely from a location very near or at the Flax Pond location. The Westport ozonesonde profile (Fig. 6e) shows two pronounced layers peaking around 500 and 2000m with significantly higher O_3 than those over Flax Pond, at nearly 110 ppb for each layer above Westport compared to 82 and 75 ppb above Flax Pond. The extremely high ozone observed at 500 m is seen to be a combination of ozone advected over LIS and that produced

395 locally from emissions and photochemistry over coastal Connecticut. The O_3 peak at around 2
396 km is above the boundary layer in an air mass that was circulating over the ocean before
397 returning north. Complementing the ozone sounding in Fig. 6e, Fig. 6d shows the vertical
398 concentration profiles of the LMOL beginning at 10 UTC, profiles of three ozonesondes at 13Z,
399 17Z, and 22Z, and the CT-DEEP surface O_3 measurements. The ozone level is seen to increase
400 during the day both above and below a relatively clean layer at 1.5 km, with the low altitude
401 ozone maximum between 500 and 1000 m persisting for hours into the night, while the surface
402 concentration decreases in the evening.

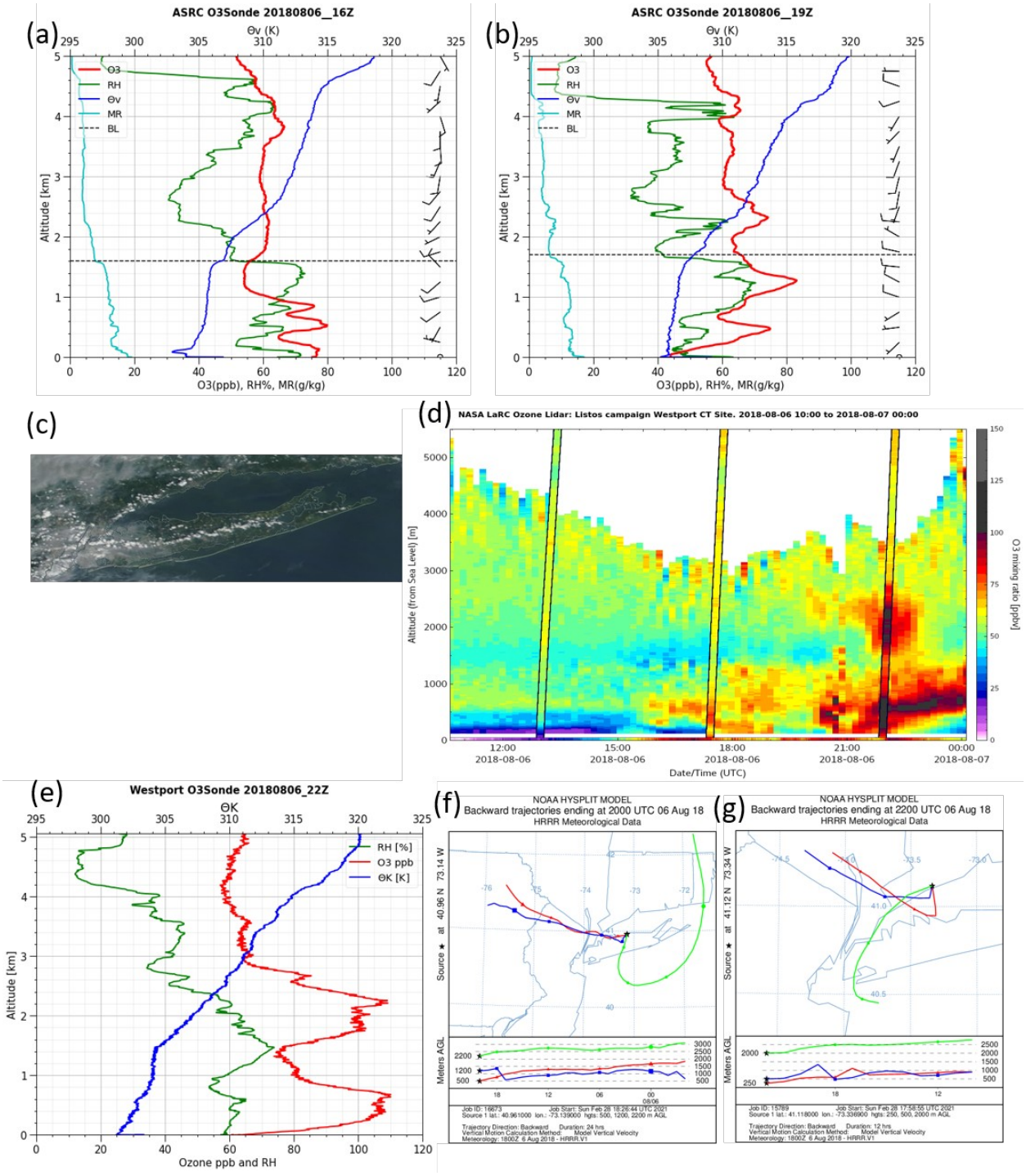

Figure 6. 6 August 2018 event. (a) Ozonesonde profile for 17Z 6 Aug 2018 (Flax Pond). (b) Ozonesonde profile for 19:46Z 6 Aug 2018 (Flax Pond). (c) NASA EOSDIS Worldview visible satellite image for Long Island on 6 Aug 2018 (https://worldview.earthdata.nasa.gov). (d) NASA LaRC ozone LiDAR curtain plot measured at Westport, CT from 10 UTC 6 Aug to 0 UTC 7 Aug 2018. Surface O3 (CT-DEEP) is shown across the bottom. Vertical profiles are shown for three ozonesondes launched at 13Z, 17Z and 22Z. (e) NASA LaRC ozonesonde profile for 22Z

411 6 Aug 2018 (Westport, CT). (f) Backward trajectory with Flax Pond as receptor site ending at 20
412 UTC on 6 Aug 2018. (g) Backward trajectory with Westport, CT as receptor site, 12 hours
413 ending at 22 UTC on 6 Aug 2018.
414

415 3.6 Convergence of Bay & Sea Breeze over LI: 28-29 July 2019

416 This two day event with temperatures well in excess of 30°C produced an $MDA8O_3$ of 79
417 ppb on 28 July, with the highest $MDA8O_3$ for the NYC metro area during 2019 of 85 ppb
418 recorded on 29 July at Flax Pond. Three ozonesondes were launched over the two day period
419 from the Stony Brook site (Table 2).

420 On 28 July, back trajectories (Fig. S8a) and LiDAR vertical winds (Fig. S8b) indicate air
421 flow from southwest and west of LI was well-mixed throughout the boundary layer, producing
422 the broad O_3 maximum of 90 ppb between 400 and 1800 m seen in the 20Z ozone vertical profile
423 (Fig. S8c).

424 The late afternoon ozone vertical profile at 19Z on 29 July (Fig 7a) shows ozone
425 increasing smoothly from 82 ppb at the surface to a single broad maximum of 102 ppb at 1200–
426 1600 m, and then tapering to 60 ppb just above the boundary layer. The 19Z back trajectory
427 indicates westerly flow at all levels in the boundary layer (Fig. 7b). The trajectories at 100 m and
428 1500 m are virtually identical, both horizontally and vertically, only diverging at 17 UTC to sink
429 over the water and rise over the land. Also note that vertical mixing strengthened throughout the
430 boundary layer from 16 to 21 UTC (Fig. S8d). Wind LiDARs show the pattern of midday
431 stagnation, with a sea-breeze at Wantagh (Fig. S8e), and shore-breeze at Stony Brook (Fig. S8f)
432 similar to those seen in the 6 August 2018 case. Satellite photography on 29 July (Fig. S8g) once
433 again shows the appearance of a line of cumulus clouds in the middle of LI due to
434 sea-breeze/shore-breeze convergence.

435 On 29 July the University of Maryland (UMD) Cessna 402B measured ozone and
436 precursors in the Long Island Sound area and provided a unique opportunity for multiple vertical
437 profile measurements in the lower troposphere in a relatively small area (approximately 150
438 km^2). Fig. 7c shows the 29 July ozonesonde profile starting at 9:13 UTC in red, the spiral up
439 profile from the Cessna starting at 19:35 UTC in magenta, and the spiral down profile from the
440 Cessna starting at 19:52 UTC in cyan. While the three profiles are very similar above 1600 m,
441 the differences at lower altitudes are striking, especially the stark difference between the up and
442 down spiral of the Cessna. The location of the plane (latitude, longitude, altitude) is shown in

Fig. 7d, while Fig. 7e shows the measured O_3 concentration. In Fig. 7e, the red trace beginning in the upper right indicates the plane came in low over the water of Long Island Sound, measuring ozone close to 120 ppb, while the ozonesonde, over land and approximately 10 km away, measured ~85 ppb. Remaining over the Sound, the plane spiraled up, still measuring high ozone to 1500 m, and then declining to about 60 ppb as it reached the maximum altitude of 2800 m. The plane then spiraled down, and the ozone increased again to over 90 pbb at 1800 m, but then settled down to values in the high 80s as the plane headed northwest back over LIS. There is a 20–25 ppb difference in the ozone mixing ratios measured between 600 and 1400m altitude during the upward spiral and the downward spiral, although they are separated by only a few km. This horizontal gradient is similar to the land-water interface gradients observed in previous work by Stauffer et al. (Stauffer et al., 2015) and Zhang et al. (Zhang et al., 2020).

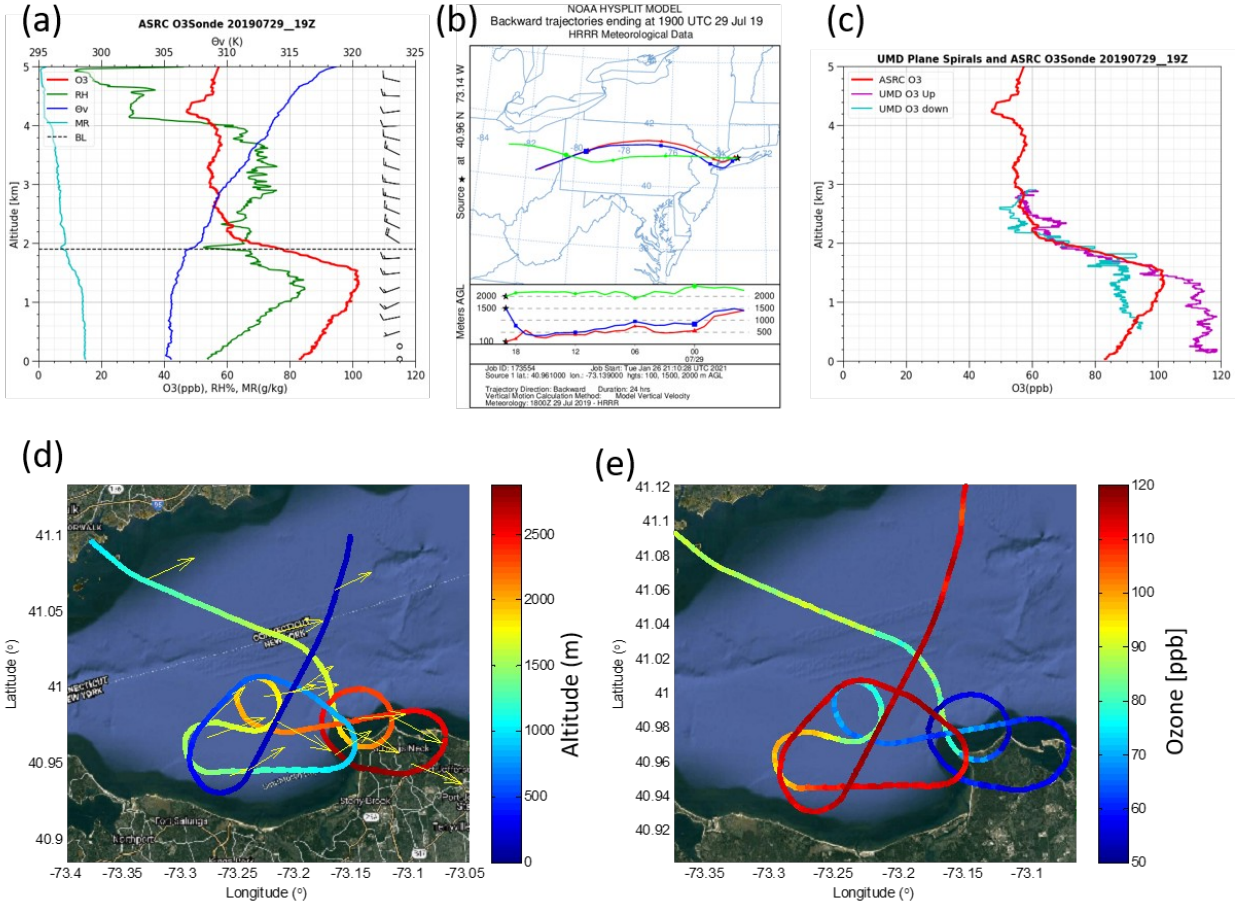

Figure 7. 28–29 July 2019 event. (a) Ozonesonde profile for 19:13Z on 29 July 2019. (b) Backward trajectory with Flax Pond as receptor site ending at 19:00 UTC on 29 July 2019. (c) Comparison of O3 vertical profiles from the 19Z 29 July 2019 sonde with measurements from the UMD plane spirals over Flax Pond (upward leg is magenta, and downward leg is cyan). (d)

Flight path and altitude of UMD plane. (e) Ozone concentrations measured by UMD plane during spiral.

4. Discussion and Conclusions

A common model for urban ozone pollution pictures enhanced precursor pollutant emissions in urban areas which are ventilated horizontally and vertically by prevailing winds. During transit, the precursors dilute through Gaussian diffusion and the in-mixing of cleaner air, all the while undergoing efficient photochemical oxidation producing enhanced ozone concentrations. Even though reactant concentrations drop, ozone production efficiency (OPE) increases as a result of the lower NO_x, so overall ozone production remains strong for tens and even hundreds of kilometers downwind (Godowitch et al., 2008; Ninneman et al., 2019) and receptor sites downwind experience higher ozone than locations in the urban center. This study focuses on and describes cases where ozone concentrations are not always smoothly varying. The cases of greatest interest involve rapid variation in ozone levels, both vertically and horizontally. To create these unusually rapid spatial variances in ozone, the influences on circulation must be far more local, too local for pollutant transport to be well described by Gaussian diffusion in a stably advecting air mass. The complicated arrangement of land and water in the NYC Metro area contributes to flow effects that can create these rapidly varying ozone air masses.

Our results indicate that vertical layering of ozone mixing ratio in the lower troposphere occurs when there is significant shear in the vertical wind profile. This makes sense intuitively, but also points out that 1) in regions with land-water interfaces the air flow is more complex and ozone production is not uniform across large areas; and 2) this heterogeneity in ozone production and small scale circulation presents itself in highly structured vertical ozone profiles on a number of warm summer days, and more occasionally as structured heterogeneity in the horizontal direction, both aloft as shown here, and at the surface as shown by others (Stauffer et al., 2015; Zhang et al., 2020). Shearing in the high ozone cases studied here was generated by a low-level jet and/or sea-breeze circulation.

A total of 26 ozonesondes were launched from the north-central Long Island locations of Flax Pond and Stony Brook during the LISTOS 2018 and 2019 campaigns. The launches provided data that is as interesting as it is often complicated. In a typical mid-latitude continental location with homogeneous land use, during mid-summer one might expect a mixed layer

extending on sunny days to 1500 m or even higher, and smoothly varying ozone throughout this mixed layer. This location on central Long Island is surrounded by two large bodies of water, the Long Island Sound to the north and the Atlantic Ocean to the south, and the atmospheric chemistry is further complicated by the large emission sources from New York City, New Jersey, and the I95 corridor less than 100 km to the west and south. In summer, all these influencing factors combine to introduce the complications referred to above. High temperatures lead to high power plant emissions from source regions and enhanced photochemical reactions; high temperatures and stable weather patterns lead to stagnation and reduced ventilation of emissions and secondary pollutants; and stagnation conditions open the door for small scale circulation processes like low-level jets and sea-breeze circulation to play a much larger, and even dominant role in pollutant transport.

Five cases were explored in greater detail to tease out, to the extent possible, how the relatively more pronounced small scale circulations intertwined with enhanced emissions and photochemistry not only to generate high ozone conditions, but high ozone conditions with marked vertical layering and/or horizontal gradient in ozone. The 18 June 2018 case provides an example of shearing and a small scale perturbation caused by a low-level jet with a resulting ozone profile at Flax Pond that increased from just below 60 ppb at the surface to over 100 ppb at 700 m altitude. The next case, concluding on 2 July 2018, was a more classic blocking high with very high temperatures and stagnation conditions for at least three days. In these conditions the high ozone took three days to migrate east all the way to Flax Pond, and the ozone profiles showed multiple layers due to sea-breeze and shore breeze flows, including air that passed over Long Island, stagnated over the Atlantic Ocean, and flowed back to Long Island as part of a well-organized sea-breeze flow. The 10 July 2018 case was marked by its extraordinarily high ozone aloft and at the surface rather than complex small scale circulation. In many ways, this day's evolution fits the "common model" described above much better than the other cases. The 6 August 2018 case is also remarkable for its complex layered structure, driven at least in part by the convergence of sea and shore-breezes over Long Island, and a corresponding shore breeze over coastal Connecticut. Very distinct layers and much higher ozone concentrations were observed at Westport, CT on this day by the NASA ozone LiDAR and ozonesonde. Last, but not least, on 29 July 2019 the ozone was concentrated in a single layer aloft, where it grew to concentrations of over 100 ppb at 1500 m altitude. Stagnation, sea and shore breezes played a

role in this build up. Very striking on this day is the ozone measurements from the UMD aircraft which passed over Flax Pond minutes after the balloon was launched from nearby Stony Brook. The up spiral over the water measured ozone 20-25 ppb greater than the down spiral some 15 minutes later and 15 km away. This illustrates that highly structured ozone profiles can occur both vertically and horizontally.

This study adds to the growing recognition that ozone pollution in the vicinity of urban areas near large bodies of water can be strongly influenced by small scale dynamics generated by the land-water interface (Dreessen et al., 2019; Goldberg et al., 2014; Sullivan et al., 2019). These land-water circulations take on added importance in hot stagnant conditions and have been shown to recirculate uncharacteristically high concentrations of ozone back onto the urban area and impact the populations there (Martins et al., 2012). As the spatial resolution of models has increase to 3 km in the horizontal (and sometimes better), the skill of predicting and diagnosing these small scale features has improved. Spatial heterogeneity, both vertical and horizontal, have likely been underestimated in models and therefore in plans for regulation and air quality improvement. Even the best models remain unable to predict and describe some of the more complexly structured profiles observed in the work. Measurements of small scale vertical and horizontal profiles of ozone and important precursors remain our only way to hope to understand the interplay of the forces described here and their fascinating complexity as they illustrate the highly structured character of the atmosphere in these situations.

Acknowledgments and Data

This work was supported through the Northeast States for Coordinated Air Use Management (NESCAUM) by the New York State Energy Research and Development Authority (NYSERDA) Master Agreement 101132. NYSERDA has not reviewed the information contained herein, and the opinions expressed in this report do not necessarily reflect those of NYSERDA or the State of New York.

Special thanks go to Paul Miller and George Allen, at NESCAUM for their direction and support throughout the project. We gratefully acknowledge the support and assistance of New York State Department of Environmental Conservation (NYS DEC), especially Mike Costello and Paul Sierzenga in Albany for loaning and transporting the trailer, and Peter Sproul, Laura Wheeler, and Michael Radesco, at Stony Brook for hosting our field site. Thanks to Stony Brook University, and especially Stephen Abrams, the curator of the Flax Pond Marine Laboratory. Many thanks to our students, Christopher Conover, and Marlena Maura for sonde preparation and launch support, and to our colleagues at ASRC and the entire LISTOS team for their support. Thanks to Russ Dickerson (UMD), Phillip Stratton (UMD), and Xinrong Ren (NOAA/ARL) for aircraft data for our 2019 case, and to Tim Berkoff (NASA), for 6 August 2018 LMOL data. The

authors gratefully acknowledge the NOAA Air Resources Laboratory (ARL) for the provision of the HYSPLIT transport and dispersion model and/or READY website (https://www.ready.noaa.gov) used in this publication. We acknowledge the use of imagery from the NASA Worldview application (https://worldview.earthdata.nasa.gov), part of the NASA Earth Observing System Data and Information System (EOSDIS). Thanks to the New York State Mesonet for LiDAR profile data (www.nysmesonet.org). Data are available online (https://www-air.larc.nasa.gov/missions/listos/index.html). The deployment of the Langley Mobile Ozone Lidar to the LISTOS campaign was made possible by funding from NASA's Tropospheric Composition Program and site support by the Connecticut's Department of Energy and Environmental Protection.

The authors declare that they have no real or perceived financial conflicts of interest.

References

Angevine, W. M., Senff, C. J., White, A. B., Williams, E. J., Koermer, J., Miller, S. T. K., et al. (2004). Coastal boundary layer influence on pollutant transport in New England. *Journal of Applied Meteorology*, *43*(10), 1425–1437. https://doi.org/10.1175/JAM2148.1

Bell, M. L., Peng, R. D., & Dominici, F. (2006). The exposure-response curve for ozone and risk of mortality and the adequacy of current ozone regulations. *Environmental Health Perspectives*, *114*(4), 532–536. https://doi.org/10.1289/ehp.8816

Bloomer, B. J., Stehr, J. W., Piety, C. A., Salawitch, R. J., & Dickerson, R. R. (2009). Observed relationships of ozone air pollution with temperature and emissions. *Geophysical Research Letters*, *36*(9), L09803. https://doi.org/10.1029/2009GL037308

Brotzge, J. A., Wang, J., Thorncroft, C. D., Joseph, E., Bain, N., Bassill, N., et al. (2020). A technical overview of the New York state mesonet standard network. *Journal of Atmospheric and Oceanic Technology*, *37*(10), 1827–1845. https://doi.org/10.1175/JTECH-D-19-0220.1

Clifton, O. E., Fiore, A. M., Massman, W. J., Baublitz, C. B., Coyle, M., Emberson, L., et al. (2020, March 1). Dry Deposition of Ozone Over Land: Processes, Measurement, and Modeling. *Reviews of Geophysics*. Blackwell Publishing Ltd. https://doi.org/10.1029/2019RG000670

Clifton, O. E., Paulot, F., Fiore, A. M., Horowitz, L. W., Correa, G., Baublitz, C. B., et al. (2020). Influence of Dynamic Ozone Dry Deposition on Ozone Pollution. *Journal of Geophysical Research: Atmospheres*, *125*(8), e2020JD032398. https://doi.org/10.1029/2020JD032398

Dacic, N., Sullivan, J. T., Knowland, K. E., Wolfe, G. M., Oman, L. D., Berkoff, T. A., & Gronoff, G. P. (2020). Evaluation of NASA's high-resolution global composition simulations: Understanding a pollution event in the Chesapeake Bay during the summer 2017 OWLETS campaign. *Atmospheric Environment*, *222*, 117133. https://doi.org/10.1016/j.atmosenv.2019.117133

Dreessen, J., Orozco, D., Boyle, J., Szymborski, J., Lee, P., Flores, A., & Sakai, R. K. (2019). Observed ozone over the Chesapeake Bay land-water interface: The Hart-Miller Island Pilot Project. *Journal of the Air & Waste Management Association*, *69*(11), 1312–1330. https://doi.org/10.1080/10962247.2019.1668497

Farris, B. M., Gronoff, G. P., Carrion, W., Knepp, T., Pippin, M., & Berkoff, T. A. (2019). Demonstration of an off-Axis parabolic receiver for near-range retrieval of lidar ozone profiles. *Atmospheric Measurement Techniques*, *12*(1), 363–370. https://doi.org/10.5194/amt-12-363-2019

Fishman, J., Bowman, K. W., Burrows, J. P., Richter, A., Chance, K. V., Edwards, D. P., et al. (2008, June 1). Remote sensing of tropospheric pollution from space. *Bulletin of the American Meteorological Society*.

599 American Meteorological Society. https://doi.org/10.1175/2008BAMS2526.1

600 Godowitch, J. M., Hogrefe, C., & Rao, S. T. (2008). Diagnostic analyses of a regional air quality model: Changes in
601 modeled processes affecting ozone and chemical-transport indicators from NO_x point source emission
602 reductions. *Journal of Geophysical Research*, *113*(D19), D19303. https://doi.org/10.1029/2007JD009537

603 Goldberg, D. L., Loughner, C. P., Tzortziou, M. A., Stehr, J. W., Pickering, K. E., Marufu, L. T., & Dickerson, R. R.
604 (2014). Higher surface ozone concentrations over the Chesapeake Bay than over the adjacent land:
605 Observations and models from the DISCOVER-AQ and CBODAQ campaigns. *Atmospheric Environment*, *84*,
606 9–19. https://doi.org/10.1016/j.atmosenv.2013.11.008

607 Gronoff, G., Robinson, J., Berkoff, T., Swap, R., Farris, B., Schroeder, J., et al. (2019). A method for quantifying
608 near range point source induced O3 titration events using Co-located Lidar and Pandora measurements.
609 *Atmospheric Environment*, *204*, 43–52. https://doi.org/10.1016/j.atmosenv.2019.01.052

610 Hu, X. M., Klein, P. M., Xue, M., Zhang, F., Doughty, D. C., Forkel, R., et al. (2013). Impact of the vertical mixing
611 induced by low-level jets on boundary layer ozone concentration. *Atmospheric Environment*, *70*, 123–130.
612 https://doi.org/10.1016/j.atmosenv.2012.12.046

613 Huang, Y., Dominici, F., & Bell, M. L. (2005). Bayesian hierarchical distributed lag models for summer ozone
614 exposure and cardio-respiratory mortality. *Environmetrics*, *16*(5), 547–562. https://doi.org/10.1002/env.721

615 Johnson, B. J. (2002). Electrochemical concentration cell (ECC) ozonesonde pump efficiency measurements and
616 tests on the sensitivity to ozone of buffered and unbuffered ECC sensor cathode solutions. *Journal of*
617 *Geophysical Research*, *107*(D19), 4393. https://doi.org/10.1029/2001JD000557

618 Kinney, P. L. (1999). The Pulmonary Effects of Outdoor Ozone and Particle Air Pollution. *Seminars in Respiratory*
619 *and Critical Care Medicine*, *20*(06), 601–607. https://doi.org/10.1055/s-2007-1009479

620 Kleiman, G. (2010). The Nature of the Ozone Air Quality Problem in the Ozone Transport Region : A Conceptual
621 Description.

622 Knowlton, K., Rosenthal, J. E., Hogrefe, C., Lynn, B., Gaffin, S., Goldberg, R., et al. (2004). Assessing ozone-
623 related health impacts under a changing climate. *Environmental Health Perspectives*, *112*(15), 1557–1563.
624 https://doi.org/10.1289/ehp.7163

625 Lamsal, L. N., Duncan, B. N., Yoshida, Y., Krotkov, N. A., Pickering, K. E., Streets, D. G., & Lu, Z. (2015). U.S.
626 NO2 trends (2005-2013): EPA Air Quality System (AQS) data versus improved observations from the Ozone
627 Monitoring Instrument (OMI). *Atmospheric Environment*, *110*, 130–143.
628 https://doi.org/10.1016/j.atmosenv.2015.03.055

629 Lee, S. H., Kim, S. W., Trainer, M., Frost, G. J., McKeen, S. A., Cooper, O. R., et al. (2011). Modeling ozone
630 plumes observed downwind of New York City over the North Atlantic Ocean during the ICARTT field
631 campaign. *Atmospheric Chemistry and Physics*, *11*(14), 7375–7397. https://doi.org/10.5194/acp-11-7375-2011

632 Levy, I., Makar, P. A., Sills, D., Zhang, J., Hayden, K. L., Mihele, C., et al. (2010). Unraveling the complex local-
633 scale flows influencing ozone patterns in the southern Great Lakes of North America. *Atmospheric Chemistry*
634 *and Physics*, *10*(22), 10895–10915. https://doi.org/10.5194/acp-10-10895-2010

635 Loughner, C. P., Allen, D. J., Pickering, K. E., Zhang, D. L., Shou, Y. X., & Dickerson, R. R. (2011). Impact of fair-
636 weather cumulus clouds and the Chesapeake Bay breeze on pollutant transport and transformation.
637 *Atmospheric Environment*, *45*(24), 4060–4072. https://doi.org/10.1016/j.atmosenv.2011.04.003

638 Martins, D. K., Stauffer, R. M., Thompson, A. M., Knepp, T. N., & Pippin, M. (2012). Surface ozone at a coastal
639 suburban site in 2009 and 2010: Relationships to chemical and meteorological processes. *Journal of*

Geophysical Research Atmospheres, *117*(5). https://doi.org/10.1029/2011JD016828

Naja, M. (2003). Ozone in background and photochemically aged air over central Europe: Analysis of long-term ozonesonde data from Hohenpeissenberg and Payerne. *Journal of Geophysical Research*, *108*(D2), 4063. https://doi.org/10.1029/2002JD002477

Ninneman, M., Demerjian, K. L., & Schwab, J. J. (2019). Ozone Production Efficiencies at Rural New York State Locations: Relationship to Oxides of Nitrogen Concentrations. *Journal of Geophysical Research: Atmospheres*, *124*(4), 2363–2376. https://doi.org/10.1029/2018JD029932

Patz, J. A. (2003). Climate change and health: new research challenges. *Managing for Healthy Ecosystems*, 77–86.

Qin, M., Yu, H., Hu, Y., Russell, A. G., Odman, M. T., Doty, K., et al. (2019). Improving ozone simulations in the Great Lakes Region: The role of emissions, chemistry, and dry deposition. *Atmospheric Environment*, *202*, 167–179. https://doi.org/10.1016/j.atmosenv.2019.01.025

Smit, H. G. J., Straeter, W., Johnson, B. J., Oltmans, S. J., Davies, J., Tarasick, D. W., et al. (2007). Assessment of the performance of ECC-ozonesondes under quasi-flight conditions in the environmental simulation chamber: Insights from the Juelich Ozone Sonde Intercomparison Experiment (JOSIE). *Journal of Geophysical Research*, *112*(D19), D19306. https://doi.org/10.1029/2006JD007308

Stauffer, R. M., Thompson, A. M., Martins, D. K., Clark, R. D., Goldberg, D. L., Loughner, C. P., et al. (2015). Bay breeze influence on surface ozone at Edgewood, MD during July 2011. *Journal of Atmospheric Chemistry*, *72*(3–4), 335–353. https://doi.org/10.1007/s10874-012-9241-6

Stehr, J., Wierman, S. S. G., & Stephenson, S. (2005). A Guide to Mid-Atlantic Regional Air Quality. *Mid-Atlantic Regional Air Management Association*. Retrieved from papers3://publication/uuid/1A4F12E2-3055-495A-ACE1-AC44BF8479C4

Stein, A. F., Draxler, R. R., Rolph, G. D., Stunder, B. J. B., Cohen, M. D., & Ngan, F. (2015, December 1). Noaa's hysplit atmospheric transport and dispersion modeling system. *Bulletin of the American Meteorological Society*. American Meteorological Society. https://doi.org/10.1175/BAMS-D-14-00110.1

Sullivan, J. T., Berkoff, T., Gronoff, G., Knepp, T., Pippin, M., Allen, D., et al. (2019). The ozone water-land environmental transition study: An innovative strategy for understanding Chesapeake Bay pollution events. *Bulletin of the American Meteorological Society*, *100*(2), 291–306. https://doi.org/10.1175/BAMS-D-18-0025.1

Tawfik, A. B., & Steiner, A. L. (2013). A proposed physical mechanism for ozone-meteorology correlations using land-atmosphere coupling regimes. *Atmospheric Environment*, *72*, 50–59. https://doi.org/10.1016/j.atmosenv.2013.03.002

Thompson, A. M., Stauffer, R. M., Miller, S. K., Martins, D. K., Joseph, E., Weinheimer, A. J., & Diskin, G. S. (2015). Ozone profiles in the Baltimore-Washington region (2006-2011): Satellite comparisons and DISCOVER-AQ observations. *Journal of Atmospheric Chemistry*, *72*(3–4), 393–422. https://doi.org/10.1007/s10874-014-9283-z

USEPA. (2013). Integrated Science Assessment (ISA) for Ozone and Related Photochemical Oxidants (Final Report, Feb 2013).

De Young, R., Carrion, W., Ganoe, R., Pliutau, D., Gronoff, G., Berkoff, T., & Kuang, S. (2017). Langley mobile ozone lidar: ozone and aerosol atmospheric profiling for air quality research. *Applied Optics*, *56*(3), 721. https://doi.org/10.1364/ao.56.000721

Zhang, J., Mak, J., Wei, Z., Cao, C., Ninneman, M., Marto, J., & Schwab, J. J. (2021). Long Island enhanced aerosol

681 event during 2018 LISTOS: Association with heatwave and marine influences. *Environmental Pollution*, *270*,
682 116299. https://doi.org/10.1016/j.envpol.2020.116299

683 Zhang, J., Ninneman, M., Joseph, E., Schwab, M. J., Shrestha, B., & Schwab, J. J. (2020). Mobile Laboratory
684 Measurements of High Surface Ozone Levels and Spatial Heterogeneity During LISTOS 2018: Evidence for
685 Sea Breeze Influence. *Journal of Geophysical Research: Atmospheres*, *125*(11), e2019JD031961.
686 https://doi.org/10.1029/2019JD031961

687